Bidirectional effects of hydrogen sulfide via ATP-sensitive K^+ channels and transient receptor potential A1 channels in RIN14B cells

Ayako Ujike, Ken-ichi Otsuguro, Ryo Miyamoto, Soichiro Yamaguchi, and Shigeo Ito

Laboratory of Pharmacology, Graduate School of Veterinary Medicine, Hokkaido University, Sapporo 060-0818, Japan

Corresponding author: K. Otsuguro, Laboratory of pharmacology, Graduate School of Veterinary medicine, Hokkaido University, Kita 18, Nishi 9, Sapporo 060-0818, Japan.
Tel. & Fax: +81-11-706-5220; E-mail address: otsuguro@vetmed.hokudai.ac.jp

Abstract

Hydrogen sulfide (H_2S) reportedly acts as a gasotransmitter because it mediates various cellular responses through several ion channels including ATP-sensitive K^+ (K_{ATP}) channels and transient receptor potential (TRP) A1 channels. H_2S can activate both K_{ATP} and TRPA1 channels at a similar concentration range. In a single cell

expressing both channels, however, it remains unknown what happens when both channels are simultaneously activated by H_2S. In this study, we examined the effects of H_2S on RIN14B cells that express both K_{ATP} and TRPA1 channels. RIN14B cells showed several intracellular Ca^{2+} concentration ($[Ca^{2+}]_i$) responses to NaHS (300 μM), an H_2S donor, i.e., inhibition of spontaneous Ca^{2+} oscillations (37%), inhibition followed by $[Ca^{2+}]_i$ increase (24%), and a rapid increase in $[Ca^{2+}]_i$ (25%). K_{ATP} channel blockers, glibenclamide or tolbutamide, abolished any inhibitory effects of NaHS and enhanced NaHS-mediated $[Ca^{2+}]_i$ increases, which were inhibited by extracellular Ca^{2+} removal, HC030031 (a TRPA1 antagonist), and disulfide bond-reducing agents. NaHS induced 5-hydroxytryptamine (5-HT) release from RIN14B cells, which was also inhibited by TRPA1 antagonists. These results indicate that H_2S has both inhibitory and excitatory effects by opening K_{ATP} and TRPA1 channels, respectively, in RIN14B cells, suggesting potential bidirectional modulation of secretory functions.

Keywords:

Hydrogen sulfide; Ca^{2+} signal; TRPA1; K_{ATP} channels; RIN14B cells

1. Introduction

Hydrogen sulfide (H_2S) reportedly acts as a gasotransmitter, like nitric oxide, carbon monoxide and ammonium (Wang, 2014). In mammals, H_2S is enzymatically synthesized from cysteine in various tissues and also produced by enterobacteria in the gastrointestinal tract (Carbonero et al., 2012; Kamoun, 2004). Many reports indicate that H_2S plays an important role in various physiological functions (Predmore et al., 2012). In addition, therapeutic drugs releasing H_2S as anti-inflammatory have been developed (Chan and Wallace, 2013; Szabó, 2007).

Various ion channels are reported as targets of H_2S (Tang et al., 2010). In sensory neurons, H_2S acts on transient receptor potential (TRP) V1 and voltage-dependent T-type Ca^{2+} channels, leading to bladder contraction and hyperalgesia, respectively (Maeda et al., 2009; Patacchini et al., 2005). We previously reported that H_2S causes excitation of sensory neurons via Ca^{2+}-permeable TRPA1 channels (Miyamoto et al., 2011), which are a member of the TRP family of non-selective cation channels activated by cold temperatures and several pungent irritants (Bandell et al., 2004; Jordt et al., 2004; Story et al., 2003). In addition to sensory neurons, TRPA1 channels are expressed in some secretory cells, such as enteroendocrine cells and pancreatic ß cells (Cao et al., 2012; Cho et al., 2014; Nozawa et al., 2009; Purhonen et al., 2008). The increase in

intracellular Ca^{2+} through TRPA1 channels is thought to be important for triggering secretion of hormones and autacoids in these cells.

Furthermore, some secretory cells also express another target molecule of H_2S, ATP-sensitive K^+ (K_{ATP}) channels (Basavappa et al., 1994; Inagaki et al., 1995), which are inward rectifying K^+ channels composed of four Kir6.x subunits (forming the pore of the channel) and four sulfonylurea receptors (SURx; auxiliary proteins). Their activity is regulated by intracellular nucleotides (ADP and ATP) and their opening results in hyperpolarization. Thus, activation of K_{ATP} channels by H_2S causes inhibitory effects, such as relaxation in the smooth muscle of blood vessels and gastrointestinal tract, and decrease insulin release from pancreatic ß cells (Yang et al., 2005; Zhao et al., 2001).

TRPA1 and K_{ATP} channels are activated by H_2S at a similar concentration range (micromolar levels) (Miyamoto et al., 2011; Yang et al., 2005; Zhao et al., 2001). However, there are no reports examining cellular responses to H_2S in single cells expressing both channels. Although H_2S reportedly exhibits excitatory and inhibitory effects on duodenal motility through different channels on different cells (Lu et al., 2014), it remains unknown what happens when different channels in a single cell are simultaneously activated by H_2S. In this study, we investigated the effects of NaHS, an H_2S donor, on RIN14B cells, a rat pancreatic δ cell line, because these cells express

TRPA1 channels (Nozawa et al., 2009) and may also express K_{ATP} channels as suggested by an electrophysiological study (Bränström et al., 1997).

2. Materials and methods

2.1. Cell culture

RIN14B cells were purchased from DS Pharma Biomedical (Osaka, Japan) and cultured in RPMI 1640 medium (Gibco/Life Technologies, Grand Island, NY, USA) supplemented with 10% fetal bovine serum, 100 U/ml penicillin, and 100 μg/ml streptomycin (all from Gibco/Life Technologies) at 37ºC in a humidified atmosphere of 5% CO_2 and 95% air.

2.2. Ca^{2+} imaging

RIN14B cells were placed on coverslips coated with poly-D-lysine and cultured for 24 h. Cells were then incubated with 10 μM fura-2 acetoxymethylester (Dojindo, Kumamoto, Japan) and 0.002% cremophor EL (Sigma-Aldrich, St. Louis, MO, USA) for 1 h at room temperature in normal solution (140 mM NaCl, 3.3 mM KH_2PO_4, 0.8 mM K_2HPO_4, 1.2 mM $CaCl_2$, 1.2 mM $MgCl_2$, 10 mM glucose, and 20 mM HEPES, pH

adjusted to 7.4 with NaOH). Fura-2 fluorescence was measured using an inverted microscope (Diaphot 300, Nikon, Tokyo, Japan) with a fluorescence ratio imaging system (ORCA-ER, Hamamatsu Photonics, Shizuoka, Japan). Cells were continuously superfused with normal solution and illuminated at 340 and 380 nm for 61.1 ms at 5 s intervals. The respective fluorescence signals (F_{340} and F_{380}) were detected at 500 nm. The intracellular calcium concentration ($[Ca^{2+}]_i$) was calculated using a Calcium Calibration Buffer Kit (Invitrogen/Life Technologies). All experiments were performed at room temperature (22–25°C).

2.3. RT-PCR

Total RNAs were extracted from RIN14B cells and rat heart as a positive control which expresses all subunits of K_{ATP} channel (Morrissey et al., 2005; Zhou et al., 2007) using TRI Reagent (Sigma-Aldrich). RIN14B cells and rat heart tissue were homogenized with TRI Reagent. Lysates were centrifuged at 12,000 × *g* for 10 min at 4°C. Supernatants were mixed with chloroform and centrifuged at 12,000 × *g* for 15 min at 4°C. The aqueous layers were collected and isopropanol was added for precipitation. After centrifugation at 12,000 × *g* for 10 min at 4°C, the pellet was washed with 75% ethanol and dissolved in RNase-free distilled water.

RNA samples were treated with DNase I (Invitrogen/Life Technologies) for 15 min at room temperature. The reaction was stopped by adding EDTA and heating at 65°C. Samples were reverse-transcribed using ReverTra Ace with Oligo dT primers (TOYOBO, Osaka, Japan).

PCR was performed with Taq DNA polymerase (Roche, Basel, Switzerland). Template cDNAs (75 ng/reaction) were mixed with dNTP (200 μM) and each primer (0.5 μM). The following primers designed to detect K_{ATP} channel subunits were used: 5′-AAGCGCAACTCTATGAGAAG-3′ (forward) and 5′-ACCAGAACTCAGCAAACTGT-3′ (reverse) for Kir6.1 (product size: 212 bp), 5′-CGCATGGTGACAGAGGAATG-3′ and 5′-GTGGAGAGGCACAACTTCGC-3′ for Kir6.2 (297 bp), 5′-TGCCAGCTCTTTGAGCATTG-3′ and 5′-AGGATGATACGGTTGAGCAGG-3′ for SUR1 (558 bp), 5′-TTGTTCGAAAGAGCAGCATAC-3′ and 5′-GCCCGCATCCATAATAGAGG-3′ for SUR2A (155 bp), 5′-TTGTTCGAAAGAGCAGCATAC-3′ and 5′-AGCAGTCAGAATGGTGTGAACC-3′ for SUR2B (152 bp), and 5′-TGTCACCAACTGGGACGATA-3′ and 5′-ACCCTCATAGATGGGCACAG-3′ for the housekeeping gene ß-actin (280 bp). Thermal cycles were performed using a PC320 system (ASTEC, Fukuoka, Japan). Samples were incubated for 1 min at 94°C (for initial denaturation) followed by 30

cycles of denaturation (30 sec, 94°C), annealing (30 sec, 55°C for Kir6.1 and SUR2A, or 58°C for Kir6.2 and SUR2B, or 60°C for SUR1 and β-actin), and elongation (30 sec, 72°C). The final elongation was 4 min at 72°C and products were cooled to 4°C. RNAs without RT were used as a negative control to examine DNA contamination.

PCR products were separated on a 1.5% agarose gel and visualized with ethidium bromide under UV illumination.

2.4. Immunostaining

RIN14B cells were placed on coverslips and cultured for 24 h. Cells were then rinsed in PBS (137 mM NaCl, 2.68 mM KCl, 10.1 mM Na_2HPO_4, and 1.76 mM KH_2PO_4, pH adjusted to 7.4 with NaOH) and fixed with 4% paraformaldehyde for 1 h at room temperature. Cells were permeabilized with 0.3% Triton X-100 in PBS for 15 min, and blocked with 10% normal donkey serum in PBS for 1 h. Cells were then incubated with a rabbit anti-TRPA1 antibody (1:200; Novus Biologicals, Littleton, CO, USA) in 2% normal donkey serum in PBS for 1 h, and further incubated with an Alexa Fluor 488-conjugated donkey anti-rabbit antibody (H+L) (1:1000; Invitrogen/Life Technologies) in PBS in the dark. Coverslips were mounted on glass slides with Dapi-Fluoromount G (SouthernBiotech, Birmingham, AL, USA). Images were captured

with a fluorescence microscope (LSM 700, Carl Zeiss, Oberkochen, Germany).

2.5. 5-Hydroxytryptamine (5-HT) release

RIN14B cells were seeded in 60 mm dishes at a density of 2–5 × 10^5 cells/ml and cultured for 48–72 h at 37°C/5% CO_2. Once the cells reached confluence, the culture medium was removed and the cells were pre-incubated with normal solution containing 2 μM fluoxetine (5-HT reuptake inhibitor) for 1 hr, and then incubated with 2 ml normal solution containing stimulants for 15 or 30 min at 37°C. The secretory responses were terminated by placing the dishes on ice. Culture supernatants were collected and centrifuged for 2 min at 800 × *g* to remove any detached cells. Perchloric acid at a final concentration of 0.4 N was added to the supernatants and the culture dishes, and the cells remaining in the dishes were scraped and collected. After centrifugation, the acidified samples were neutralized with K_2HPO_4. After the removal of potassium percolate, clear supernatants were analyzed on a high-performance liquid chromatography (HPLC) system equipped with an electrochemical detector. The mobile phase consisted of a citric acid buffer (0.1 M citric acid, 0.1 M sodium acetate; pH 3.5), 19% methanol, 5 mg/l EDTA-2Na, and 190 mg/l 1-octanesulfonic acid. The mobile phase was degased and perfused at 0.5 ml/min. Samples (50 μl) were injected with an

1 autosampler (Model 33, System Instruments, Tokyo, Japan), and the 5-HT in the
2 sample was separated on an octadecylsilane column (EICOMPAK SC-5ODS, 3.0 × 150
3 mm, EICOM, Kyoto, Japan) kept at 30ºC. Detection of 5-HT was performed at +450 mV
4 with an electrochemical detector (ECD-300, EICOM), and the area under the 5-HT peak
5 was measured. The ratio of 5-HT release (%) was determined by dividing the amount of
6 5-HT in the supernatant by the total 5-HT (5-HT in the supernatant plus the 5-HT in
7 the cells).
8
9 *2.6. Materials*
10 Sodium hydrosulfide (NaHS) was purchased from Strem Chemicals (Newburyport,
11 MA, USA). Allyl isothiocyanate (mustard oil), dithiothreitol (DTT), and ruthenium red
12 were from Wako Pure Chemical Industries (Osaka, Japan). HC030031,
13 iodoresiniferatoxin, SB366791, and fluoxetine hydrochloride were from Tocris (Bristol,
14 UK). Tris-(2-carboxyethyl)phosphine hydrochloride (TCEP) was from Nacalai Tesque
15 (Kyoto, Japan). ω-Conotoxin GVIA and ω-agatoxin IVA were from Peptide Institute
16 (Osaka, Japan). Tolbutamide and mibefradil dihydrochloride hydrate were from
17 Sigma-Aldrich (St. Louis, MO, USA). Glibenclamide was from Funakoshi (Tokyo,
18 Japan).

2.7. Data analyses

Results are expressed as the means ± S. E. M. (n = number of independent measurements). Statistical comparisons between two groups were made using an unpaired Student's *t*-test. For multiple comparisons, ANOVA followed by Dunnett's test was used. A *P*-value of less than 0.05 was considered significant. The area under the curve (AUC) for $[Ca^{2+}]_i$ and the EC_{50} were calculated with Origin software (OriginLab, Northampton, MA, USA).

3. Results

3.1 Patterns of intracellular Ca^{2+} concentration changes in response to H_2S

The effects of NaHS, an H_2S donor, on intracellular Ca^{2+} concentration ($[Ca^{2+}]_i$) were examined in RIN14B cells. Most RIN14B cells showed spontaneous Ca^{2+} oscillations under resting conditions. In 19 of 51 cells, NaHS (300 μM) inhibited the spontaneous responses (Fig. 1A and D). However, NaHS increased $[Ca^{2+}]_i$ in 25 of 51 cells, and in half of them (12 of 25 cells), the NaHS-induced $[Ca^{2+}]_i$ increase was preceded by inhibition of the spontaneous Ca^{2+} oscillations (Fig. 1B, C and D). The percentage of cells showing

inhibition or increases in $[Ca^{2+}]_i$ were plotted against NaHS concentration (Fig. 1E). Cells producing NaHS-induced $[Ca^{2+}]_i$ increases preceded by inhibition were counted twice as cells in both categories. The percentage of cells exhibiting NaHS-induced inhibition showed a bell-shaped concentration dependence with a maximum at 300 μM. NaHS also increased $[Ca^{2+}]_i$ in a concentration-dependent manner. High concentrations of NaHS (3 mM) rapidly increased $[Ca^{2+}]_i$ without inhibition in almost all cells, but it may include Ca^{2+} increase by toxic effect of high concentration of H_2S. These results indicate that H_2S has both inhibitory and excitatory effects on $[Ca^{2+}]_i$ signals in RIN14B cells.

3.2. Effects of K_{ATP} channel blockers on Ca^{2+} responses to H_2S

RIN14B cells reportedly express K_{ATP} channel subtypes as determined by an electrophysiological approach (Bränström et al., 1997). Thus, the expression of K_{ATP} channel subtypes in RIN14B cells was first investigated with RT-PCR. RIN14B cells expressed mRNA encoding Kir6.2 and SUR1, subunits of K_{ATP} channels, but not Kir6.1, SUR2A, and 2B (Fig. 2A). Then, the effects of K_{ATP} channel blockers, glibenclamide and tolbutamide, on the inhibition of $[Ca^{2+}]_i$ signals by NaHS were examined (Fig. 2B and C). High concentration of glibenclamide reportedly activates TRPA1 channels (Babes et al.,

2013). Therefore, we used glibenclamide at a low concentration (1 μM), which does not activate TRPA1. Although spontaneous Ca^{2+} oscillations were not affected by glibenclamide (1 μM), they were increased by tolbutamide (400 μM). In the presence of glibenclamide, NaHS (300 μM) rapidly increased $[Ca^{2+}]_i$ in almost all cells without any inhibitory effects. Similar results were obtained with tolbutamide.

As shown in Fig. 2D and E, the areas under the curve of $[Ca^{2+}]_i$ were increased by the application of NaHS alone for 10 min, but not for 2 min. In the presence of glibenclamide, however, application of NaHS for 2 min increased $[Ca^{2+}]_i$ in a concentration-dependent manner, and $[Ca^{2+}]_i$ increases induced by NaHS (10 min) were markedly enhanced. These results indicate that the K_{ATP} channel-mediated inhibitory effects of H_2S substantially masked the excitatory effects of H_2S.

3.3. Effects of Ca^{2+}-permeable channel blockers on Ca^{2+} increase by H_2S

The increase in $[Ca^{2+}]_i$ by NaHS (300 μM) was almost abolished by the removal of external Ca^{2+} with EGTA (1 mM), indicating that H_2S induced Ca^{2+} influx from the extracellular environment (Fig. 3A and B). To investigate the pathway of Ca^{2+} influx, we examined the effects of Ca^{2+}-permeable TRP channel antagonists on $[Ca^{2+}]_i$ responses to NaHS. As mRNA expression of TRPA1 in RIN14B cells was reported by Nozawa et al.

(2009), we confirmed with immunostaining that all RIN14B cells expressed TRPA1 (Fig. 3C). The increase in $[Ca^{2+}]_i$ induced by NaHS (300 μM) was inhibited by ruthenium red (a non-selective TRP antagonist, 10 μM) and HC030031 (a selective TRPA1 antagonist, 30 μM), but not by iodoresiniferatoxin (a selective TRPV1 antagonist, 100 nM) (Fig. 3D and E). These results suggest that H_2S activates TRPA1 to increase $[Ca^{2+}]_i$ in RIN14B cells.

RIN14B cells responded to BayK8644, an L-type Ca^{2+} channel agonist, suggesting the expression of L-type Ca^{2+} channels (data not shown). To investigate the involvement of voltage-dependent Ca^{2+} channels (VDCCs) in the NaHS-induced Ca^{2+} influx, the effects of VDCC blockers were examined. All Ca^{2+} channel blockers tested (1 μM ω-conotoxin, 0.1 μM ω-agatoxin, 3 μM mibefradil, and 10 μM diltiazem) failed to inhibit the increase in $[Ca^{2+}]_i$ in response to NaHS (Fig. 3F).

TRPA1 is thought to be activated via covalent cysteine modification by electrophiles (Hinman et al., 2006 and Macpherson et al., 2007). Therefore, we examined the effects of reducing agents, which were expected to inhibit formation of disulfide bonds in TRPA1. In RIN14B cells, the NaHS-induced $[Ca^{2+}]_i$ increase was also attenuated by the reducing agents dithiothreitol (DTT, 1 mM) and tris-(2-carboxyethyl)phosphine (TCEP, 1 mM) (Fig. 3G).

3.4. Effects of H_2S on 5-HT release

RIN14B cells reportedly release 5-HT via TRPA1 activation (Nozawa et al., 2009). The ability of H_2S to induce 5-HT release from RIN14B cells was therefore examined. Application of NaHS for 30 min induced 5-HT secretion in a concentration-dependent manner with an EC_{50} value of 70 μM (Fig. 4A). Glibenclamide did not significantly affect NaHS-induced 5-HT release (Fig. 4B). NaHS-induced (300 μM) 5-HT release was inhibited by HC030031 (30 μM) and DTT (1 mM), but not by TCEP (1 mM) (Fig. 4C and D).

4. Discussion

The present study demonstrated that H_2S caused both inhibitory and excitatory effects on Ca^{2+} signals in RIN14B cells, i.e., inhibition of spontaneous Ca^{2+} oscillations via K_{ATP} channels and $[Ca^{2+}]_i$ increases through TRPA1 channels resulting in 5-HT release. There are a few reports about the bidirectional effect of H_2S, especially on single cells. In the present experiment using RIN14B cells expressing K_{ATP} and TRPA1 channels, both inhibitory and excitatory effects of H_2S were observed in single cells, which suggest that H_2S may act as a bidirectional modulator for secretory functions.

Inhibition of Ca^{2+} oscillations by H_2S may be caused by opening of K_{ATP} channels, which produces hyperpolarization, because this effect was blocked by K_{ATP} channel blockers. H_2S causes relaxation of smooth muscle and decreases insulin release through K_{ATP} channel opening (Yang et al., 2005; Zhao et al., 2001). In RIN14B cells, K_{ATP} channel activity was previously recorded by electrophysiological techniques (Bränström et al., 1997). In this study, we identified the expression of the Kir6.2 and SUR1 subunits of K_{ATP} channels, like in pancreatic ß cells (Gribble et al., 1998). The combination of Kir6.x and SURx contributes to the pharmacological characteristics of these channels, such as sensitivity to sulfonylureas. The combination of Kir6.2/SUR1 is more sensitive to sulfonylureas including glibenclamide and tolbutamide than other subunits (Aguilar-Bryan et al., 1995). This is the case in RIN14B cells where these agents also effectively attenuated the NaHS-induced inhibition. H_2S reportedly interacts with cysteine residue in the extracellular loop of SUR1 subunit (Jiang et al., 2010), suggesting the direct activation of K_{ATP} channel in RIN14B cells.

A body of evidence suggests that K_{ATP} channels and VDCCs are involved in Ca^{2+} oscillations in pancreatic ß cells (Kanno et al., 2002; Liu et al., 2004). Gating of K_{ATP} channels is inhibited by intracellular ATP, which depolarizes the membrane potential, resulting in Ca^{2+} influx through VDCCs. Since L-type Ca^{2+} channel agonists increased

$[Ca^{2+}]_i$ and its blockers inhibited spontaneous Ca^{2+} oscillation in RIN14B cells (data not shown), we speculate that L-type Ca^{2+} channels are also involved in Ca^{2+} oscillations in addition to K_{ATP} channels. Hyperpolarization mediated via H_2S-induced K_{ATP} channel opening might attenuate Ca^{2+} oscillations through the inhibition of L-type Ca^{2+} channels.

In contrast to the inhibitory effect on Ca^{2+} oscillations, H_2S also increased $[Ca^{2+}]_i$ in RIN14B cells. In rat sensory neurons, we have previously reported that H_2S activates TRPA1 to increase $[Ca^{2+}]_i$ (Miyamoto et al., 2011). Activation of TRPV1 or T-type Ca^{2+} channels may also be involved in H_2S signaling (Patacchini et al., 2005; Maeda et al., 2009). However, this is not the case in RIN14B cells because the $[Ca^{2+}]_i$ response to NaHS was inhibited by a TRPA1 antagonist but not by TRPV1 antagonists or Ca^{2+} channel blockers. In addition, we confirmed TRPA1 protein expression in RIN14B cells by immunostaining. Taken together, we conclude that the excitatory effects of H_2S are mediated via TRPA1 channels in RIN14B cells.

Reducing agents inhibited $[Ca^{2+}]_i$ responses to NaHS. This suggests that TRPA1 activation by H_2S is associated with the oxidation of cysteine residues. Since the sulfur atom of H_2S is in the lowest oxidation state, formation of disulfide bonds in TRPA1 may be caused by sulfane sulfur (the chemically unstable form) of polysulfide generated from

H_2S (Greiner et al., 2013; Toohey, 2011). Otherwise, reducing agents may inhibit the oxidation of H_2S to polysulfide. The inhibitory effect of TCEP was weaker than that of DTT, although TCEP is a more potent reductant than DTT. This may be due to the lower membrane permeability of TCEP than that of DTT (Cline et al., 2004). The cysteine residues of TRPA1 that are required for activation via covalent modification by electrophilic reactive compounds are positioned in the intracellular domain (Hinman et al., 2006; Macpherson et al., 2007). This may be the site of action of H_2S. If so, it is likely that TCEP may not be able to adequately reach the site of action of H_2S and/or its derived polysulfides, or may fail to inhibit the oxidation of H_2S to polysulfide by intracellular oxidants.

NaHS-induced $[Ca^{2+}]_i$ increases became rapid and large in the presence of K_{ATP} channel blockers. This was thought to result from the cancellation of the inhibitory effects of H_2S via K_{ATP} channels and indicates that the inhibitory effects were masked during the $[Ca^{2+}]_i$ increase and occur, in a similar manner to the excitatory effects, even at high concentrations of H_2S. Application of NaHS for over 15 min only increased 5-HT release, which was not enhanced by glibenclamide. In the 5-HT release experiments, the NaHS incubation time may have been long enough for the excitatory effects to completely mask the inhibitory effects. Since inhibitory effect of H_2S tends to precede

Ca^{2+} increase as shown in Fig. 1B, further experiment will be needed to analyze the change of 5-HT release in a shorter time with high temporal resolution. In mammalian tissues, endogenous H_2S is thought to exist at quite low concentrations (Wintner et al., 2010). However, H_2S and its producing enzymes reportedly increase under pathological conditions, such as colitis and diabetes (Wallace et al., 2009; Wu et al., 2009). Increased H_2S production could result in excess release of hormones or autacoids through TRPA1, causing abnormal tissue responses.

The $[Ca^{2+}]_i$ responses to H_2S in RIN14B cells showed several patterns depending on the individual cell. This may be due to differences in expression levels of K_{ATP} and TRPA1 channels in each cell, which influences the preference for the excitatory or inhibitory effect of H_2S. The expression of these channels is reported to change under inflammatory conditions (Hatano et al., 2012; Jin et al., 2004; Kun et al., 2014). Further research is needed to examine the changes in the bidirectional effects of H_2S under pathological conditions.

Acknowledgements

This work was supported by a Grant-in-Aid for Scientific Research from the Japan Society for the Promotion of Science (No. 23658230 to K.O.).

References

Aguilar-Bryan, L., Nichols, C.G., Wechsler, S.W., Clement, J.P., Boyd, A.E., González, G., Herrera-Sosa, H., Nguy, K., Bryan, J., Nelson, D.A., 1995. Cloning of the beta cell high-affinity sulfonylurea receptor: a regulator of insulin secretion. Science 268, 423-426.

Babes, A., Fischer, M.J., Filipovic, M., Engel, M.A., Flonta, M.L., Reeh, P.W., 2013. The anti-diabetic drug glibenclamide is an agonist of the transient receptor potential Ankyrin 1 (TRPA1) ion channel. Eur. J. Pharmacol. 704, 15-22.

Bandell, M., Story, G.M., Hwang, S.W., Viswanath, V., Eid, S.R., Petrus, M.J., Earley, T.J., Patapoutian, A., 2004. Noxious cold ion channel TRPA1 is activated by pungent compounds and bradykinin. Neuron 41, 849-857.

Basavappa, S., Liddle, R.A., Mangel, A.W., 1994. Characterization of ATP-sensitive potassium channels in intestinal, cholecystokinin-secreting cells. Biochem. Biophys. Res.

Commun. 204, 855-860.

Bränström, R., Höög, A., Wahl, M.A., Berggren, P.O., Larsson, O., 1997. RIN14B: a pancreatic delta-cell line that maintains functional ATP-dependent K^+ channels and capability to secrete insulin under conditions where it no longer secretes somatostatin. FEBS Lett. 411, 301-307.

Cao, D.S., Zhong, L., Hsieh, T.H., Abooj, M., Bishnoi, M., Hughes, L., Premkumar, L.S., 2012. Expression of Transient Receptor Potential Ankyrin 1 (TRPA1) and Its Role in Insulin Release from Rat Pancreatic Beta Cells. PLoS ONE 7, e38005.

Carbonero, F., Benefiel, A.C., Gaskins, H.R., 2012. Contributions of the microbial hydrogen economy to colonic homeostasis. Nat. Rev. Gastroenterol. Hepatol. 9, 504-518.

Chan, M.V., Wallace, J.L., 2013. Hydrogen sulfide-based therapeutics and gastrointestinal diseases: translating physiology to treatments. Am. J. Physiol. Gastrointest. Liver Physiol. 305, G467-473.

Cho, H.J., Callaghan, B., Bron, R., Bravo, D.M., Furness, J.B., 2014. Identification of enteroendocrine cells that express TRPA1 channels in the mouse intestine. Cell Tissue Res. 356, 77-82.

Cline, D.J., Redding, S.E., Brohawn, S.G., Psathas, J.N., Schneider, J.P., Thorpe, C., 2004. New water-soluble phosphines as reductants of peptide and protein disulfide bonds: reactivity and membrane permeability. Biochemistry 43, 15195-15203.

Greiner, R., Pálinkás, Z., Bäsell, K., Becher, D., Antelmann, H., Nagy, P., Dick, T.P., 2013. Polysulfides link H_2S to protein thiol oxidation. Antioxid. Redox Signal. 19, 1749-1765.

Gribble, F.M., Tucker, S.J., Seino, S., Ashcroft, F.M., 1998. Tissue specificity of sulfonylureas: studies on cloned cardiac and beta-cell K_{ATP} channels. Diabetes 47, 1412-1418.

Hatano, N., Itoh, Y., Suzuki, H., Muraki, Y., Hayashi, H., Onozaki, K., Wood, I.C., Beech, D.J., Muraki, K., 2012. Hypoxia-inducible factor-1α (HIF1α) switches on transient receptor potential ankyrin repeat 1 (TRPA1) gene expression via a hypoxia response

element-like motif to modulate cytokine release. J. Biol. Chem. 287, 31962-31972.

Hinman, A., Chuang, H.H., Bautista, D.M., Julius, D. 2006. TRP channel activation by reversible covalent modification. Proc. Natl. Acad. Sci. U S A 103, 19564-19568.

Inagaki, N., Tsuura, Y., Namba, N., Masuda, K., Gonoi, T., Horie, M., Seino, Y., Mizuta, M., Seino, S., 1995. Cloning and functional characterization of a novel ATP-sensitive potassium channel ubiquitously expressed in rat tissues, including pancreatic islets, pituitary, skeletal muscle, and heart. J. Biol. Chem. 270, 5691-5694.

Jiang, B., Tang, G., Cao, K., Wu, L., Wang, R., 2010. Molecular mechanism for H_2S-induced activation of K_{ATP} channels. Antioxid. Redox Signal. 12, 1167-1178.

Jin, X., Malykhina, A.P., Lupu, F., Akbarali, H.I., 2004. Altered gene expression and increased bursting activity of colonic smooth muscle ATP-sensitive K^+ channels in experimental colitis. Am. J. Physiol. Gastrointest. Liver Physiol. 287, G274-G285.

Jordt, S.E., Bautista, D.M., Chuang, H.H., McKemy, D.D., Zygmunt, P.M., Högestätt,

E.D., Meng, I.D., Julius, D., 2004. Mustard oils and cannabinoids excite sensory nerve fibres through the TRP channel ANKTM1. Nature 427, 260-265.

Kamoun, P., 2004. Endogenous production of hydrogen sulfide in mammals. Amino Acids 26, 243-254.

Kaneko, Y., Kimura, T., Taniguchi, S., Souma, M., Kojima, Y., Kimura, Y., Kimura, H., Niki, I., 2009. Glucose-induced production of hydrogen sulfide may protect the pancreatic beta-cells from apoptotic cell death by high glucose. FEBS Lett. 583, 377-382.

Kanno, T., Rorsman, P., Göpel, S.O., 2002. Glucose-dependent regulation of rhythmic action potential firing in pancreatic ß-cells by K_{ATP}-channel modulation. J. Physiol. 545, 501-507.

Kun, J., Szitter, I., Kemény, A., Perkecz, A., Kereskai, L., Pohóczky, K., Vincze, A., Gódi, S., Szabó, I., Szolcsányi, J., Pintér, E., Helyes, Z., 2014. Upregulation of the transient receptor potential ankyrin 1 ion channel in the inflamed human and mouse colon and its protective roles. PLoS One 9, e108164.

Liu, G., Hilliard, N., Hockerman, G.H., 2004. $Ca_v1.3$ is preferentially coupled to glucose-induced $[Ca^{2+}]_i$ oscillations in the pancreatic ß cell line INS-1. Mol. Pharmacol. 65, 1269-1277.

Lu, W., Li, J., Gong, L., Xu, X., Han, T., Ye, Y., Che, T., Luo, Y., Li, J., Zhan, R., Yao, W., Liu, K., Cui, S., Liu, C., 2014. H_2S modulates duodenal motility in male rats via activating TRPV1 and K_{ATP} channels. Br. J. Pharmacol. 171, 1534-1550.

Macpherson, L.J., Dubin, A.E., Evans, M.J., Marr, F., Schultz, P.G., Cravatt, B.F., Patapoutian, A., 2007. Noxious compounds activate TRPA1 ion channels through covalent modification of cysteines. Nature 445, 541-545.

Maeda, Y., Aoki, Y., Sekiguchi, F., Matsunami, M., Takahashi, T., Nishikawa, H., Kawabata, A., 2009. Hyperalgesia induced by spinal and peripheral hydrogen sulfide: evidence for involvement of $Ca_v3.2$ T-type calcium channels. Pain 142, 127-132.

Miyamoto, R., Otsuguro, K., Ito, S., 2011. Time- and concentration-dependent activation

of TRPA1 by hydrogen sulfide in rat DRG neurons. Neurosci. Lett. 499, 137-142.

Morrissey, A., Rosner, E., Lanning, J., Parachuru, L., Dhar, Chowdhury, P., Han, S., Lopez, G., Tong, X., Yoshida, H., Nakamura, T.Y., Artman, M., Giblin, J.P., Tinker, A., Coetzee, W.A., 2005. Immunolocalization of K_{ATP} channel subunits in mouse and rat cardiac myocytes and the coronary vasculature. BMC Physiol. 5, 1.

Nozawa, K., Kawabata-Shoda, E., Doihara, H., Kojima, R., Okada, H., Mochizuki, S., Sano, Y., Inamura, K., Matsushime, H., Koizumi, T., Yokoyama, T., Ito, H., 2009. TRPA1 regulates gastrointestinal motility through serotonin release from enterochromaffin cells. Proc. Natl. Acad. Sci. U S A. 106, 3408-3413.

Patacchini, R., Santicioli, P., Giuliani, S., Maggi, C.A., 2005. Pharmacological investigation of hydrogen sulfide (H_2S) contractile activity in rat detrusor muscle. Eur. J. Pharmacol. 509, 171-177.

Predmore, B.L., Lefer, D.J., Gojon, G., 2012. Hydrogen sulfide in biochemistry and medicine. Antioxid. Redox Signal. 17, 119-140.

Purhonen, A.K., Louhivuori, L.M., Kiehne, K., Kerman, K.E., Herzig, K.H., 2008. TRPA1 channel activation induces cholecystokinin release via extracellular calcium. FEBS Lett. 582, 229-232.

Story, G.M., Peier, A.M., Reeve, A.J., Eid, S.R., Mosbacher, J., Hricik, T.R., Earley, T.J., Hergarden, A.C., Andersson, D.A., Hwang, S.W., McIntyre, P., Jegla, T., Bevan, S., Patapoutian, A., 2003. ANKTM1, a TRP-like channel expressed in nociceptive neurons, is activated by cold temperatures. Cell 112, 819-829.

Szabó, C., 2007. Hydrogen sulphide and its therapeutic potential. Nat. Rev. Drug Discov. 6, 917-935.

Tang, G., Wu, L., Wang, R., 2010. Interaction of hydrogen sulfide with ion channels. Clin. Exp. Pharmacol. Physiol. 37, 753-763.

Toohey, J.I., 2011. Sulfur signaling: is the agent sulfide or sulfane? Anal. Biochem. 413, 1-7.

Wallace, J.L., Vong, L., McKnight, W., Dicay, M., Martin, G.R., 2009. Endogenous and exogenous hydrogen sulfide promotes resolution of colitis in rats. Gastroenterology 137, 569-578.

Wang, R., 2014. Gasotransmitters: growing pains and joys. Trends Biochem. Sci. 39, 227-232.

Wintner, E.A., Deckwerth, T.L., Langston, W., Bengtsson, A., Leviten, D., Hill, P., Insko, M.A., Dumpit, R., VandenEkart, E., Toombs, C.F., Szabo, C., 2010. A monobromobimane-based assay to measure the pharmacokinetic profile of reactive sulphide species in blood. Br. J. Pharmacol. 160, 941-957.

Wu, L., Yang, W., Jia, X., Yang, G., Duridanova, D., Cao, K., Wang, R., 2009. Pancreatic islet overproduction of H_2S and suppressed insulin release in Zucker diabetic rats. Lab. Invest. 89, 59-67.

Yang, W., Yang, G., Jia, X., Wu, L., Wang, R., 2005. Activation of K_{ATP} channels by H_2S

in rat insulin-secreting cells and the underlying mechanisms. J. Physiol. 569, 519-531.

Zhao, W., Zhang, J., Lu, Y., Wang, R., 2001. The vasorelaxant effect of H_2S as a novel endogenous gaseous K_{ATP} channel opener. EMBO J. 20, 6008-6016.

Zhou, M., He, H.J., Suzuki, R., Liu, K.X., Tanaka, O., Sekiguchi, M., Itoh, H., Kawahara, K., Abe, H.J., 2007. Localization of sulfonylurea receptor subunits, SUR2A and SUR2B, in rat heart. Histochem. Cytochem. 55, 795-804.

Figure Legends

Fig. 1. Patterns of $[Ca^{2+}]_i$ responses to H_2S

(A-C) Representative patterns of $[Ca^{2+}]_i$ responses to NaHS (300 μM for 10 min). (A) Spontaneous Ca^{2+} oscillations were inhibited (Inhibition). (B) After inhibition, $[Ca^{2+}]_i$ slowly increased (Inhibition+Increase). (C) $[Ca^{2+}]_i$ rapidly increased without inhibition (Increase). (D) The percentages of cells showing each $[Ca^{2+}]_i$ response to NaHS (300 μM, n=51). (E) Concentration-dependence of NaHS-induced inhibition (○) and $[Ca^{2+}]_i$ increases (■) (n=28-51). Cells showing "Increase+Inhibition" were included in both

categories.

Fig. 2. Effects of K_{ATP} channel blockers on $[Ca^{2+}]_i$ responses to H_2S

(A) K_{ATP} channel subunit mRNA expression in RIN14B cells or rat heart (positive control). RT +/- indicates samples reverse-transcribed (+) or not (-). (B) Representative traces of $[Ca^{2+}]_i$ responses to NaHS (300 μM for 10 min) in the presence of glibenclamide (1 μM; Glib, upper trace) or tolbutamide (400 μM; Tol, lower trace). (C) The percentage of cells showing each $[Ca^{2+}]_i$ response to NaHS (300 μM) in the absence (NaHS, n=51) or presence of K_{ATP} channel blockers (NaHS+Glib, n=49 or Tol, n=56). (D, E) The relationship between NaHS concentration and area under the curve (AUC) of the $[Ca^{2+}]_i$ responses to the application of NaHS for 2 min (D) or 10 min (E). NaHS was applied in the absence (●, n=15-37) or presence (○, n=41-49) of glibenclamide (1 μM).

Fig. 3. Effect of removal of extracellular Ca^{2+}, TRP channel antagonists, and reducing agents on the H_2S-induced $[Ca^{2+}]_i$ increase

(A) Representative traces of $[Ca^{2+}]_i$ responses in the presence (cont) or absence (Ca^{2+} removal) of extracellular Ca^{2+} during the application of NaHS for 10 min. The dashed line indicates the basal $[Ca^{2+}]_i$ level before NaHS application. The Δ_1 and Δ_2 indicate

the $[Ca^{2+}]_i$ increment from the basal level at 5 and 7 min, respectively, after NaHS application. (B) Summarized data for the ratio of Δ_2 to Δ_1 (Δ_2/Δ_1) in the presence (cont; n = 31) or absence (Ca^{2+} removal; n = 33) of extracellular Ca^{2+}. *P< 0.05 vs. control (unpaired Student's *t*-test). (C) Immunostaining of RIN14B cells with an anti-TRPA1 antibody (green) and DAPI (blue). Right panels are transmission images. Upper images are negative controls without the primary antibody. (D) Representative traces of $[Ca^{2+}]_i$ responses in the absence (cont) or presence of HC030031 (HC, 30 μM) or iodoresiniferatoxin (I-RTX, 100 nM) during the application of NaHS for 10 min. (E-G) Summarized data for Δ_2/Δ_1 in the absence (cont) or presence of ruthenium red (RR, 10 μM, n = 44), HC030031 (HC, 30 μM, n = 47), iodoresiniferatoxin (I-RTX, 100 nM, n = 36), ω-conotoxin (ω-ctx, 1 μM, n = 36), ω-agatoxin (ω-atx, 0.1 μM, n = 32), mibefradil (mib, 3 μM, n=36), diltiazem (dilti, 10 μM, n=48), DTT (1 mM, n = 47), or TCEP (1 mM, n = 56). *P< 0.05 vs. cont (Dunnett's test).

Fig. 4. H_2S-induced 5-HT release from RIN14B cells.

(A) Concentration-response curve of NaHS-induced 5-HT release for 30 min. Basal release in the absence of NaHS was 7.3±0.8%. (B) 5-HT release at each NaHS concentration for 15 min in the absence or presence of glibenclamide. (C-D) The effect of

HC030031 (30 μM) (C, n = 9), DTT (1 mM), or TCEP (1 mM) (D, n = 12) on NaHS-induced 5-HT release. The release of 5-HT was normalized to the control in the absence of NaHS. *P< 0.05 (Dunnett's test).

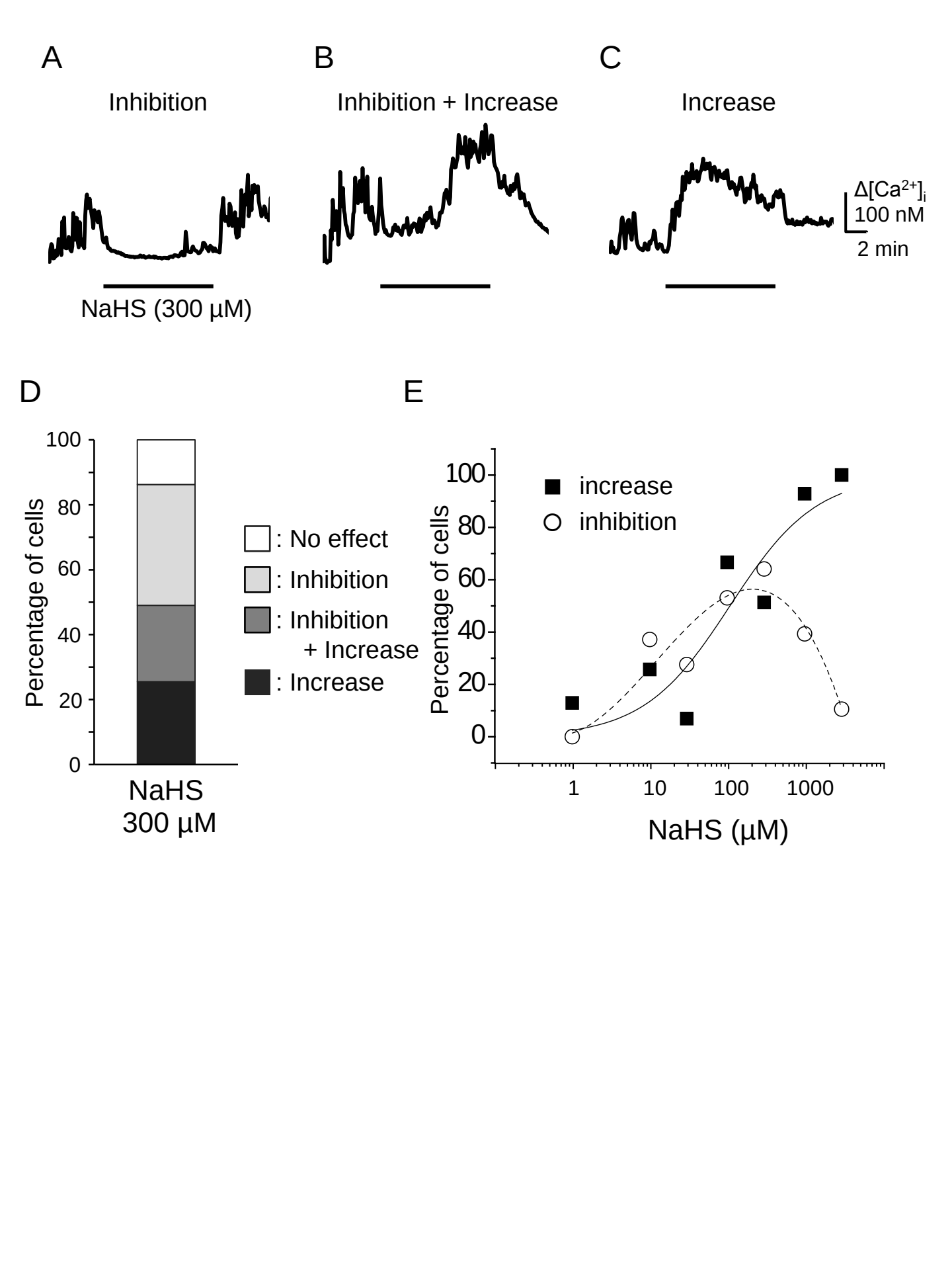
A
Inhibition
B
Inhibition + Increase
C
Increase
Δ[Ca2+]i
100 nM
2 min
NaHS (300 μM)
D
Percentage of cells
100
80
60
40
20
0
: No effect
: Inhibition
: Inhibition
+ Increase
: Increase
NaHS
300 μM
E
increase
inhibition
Percentage of cells
100
80
60
40
20
0
1
10
100
1000
NaHS (μM)

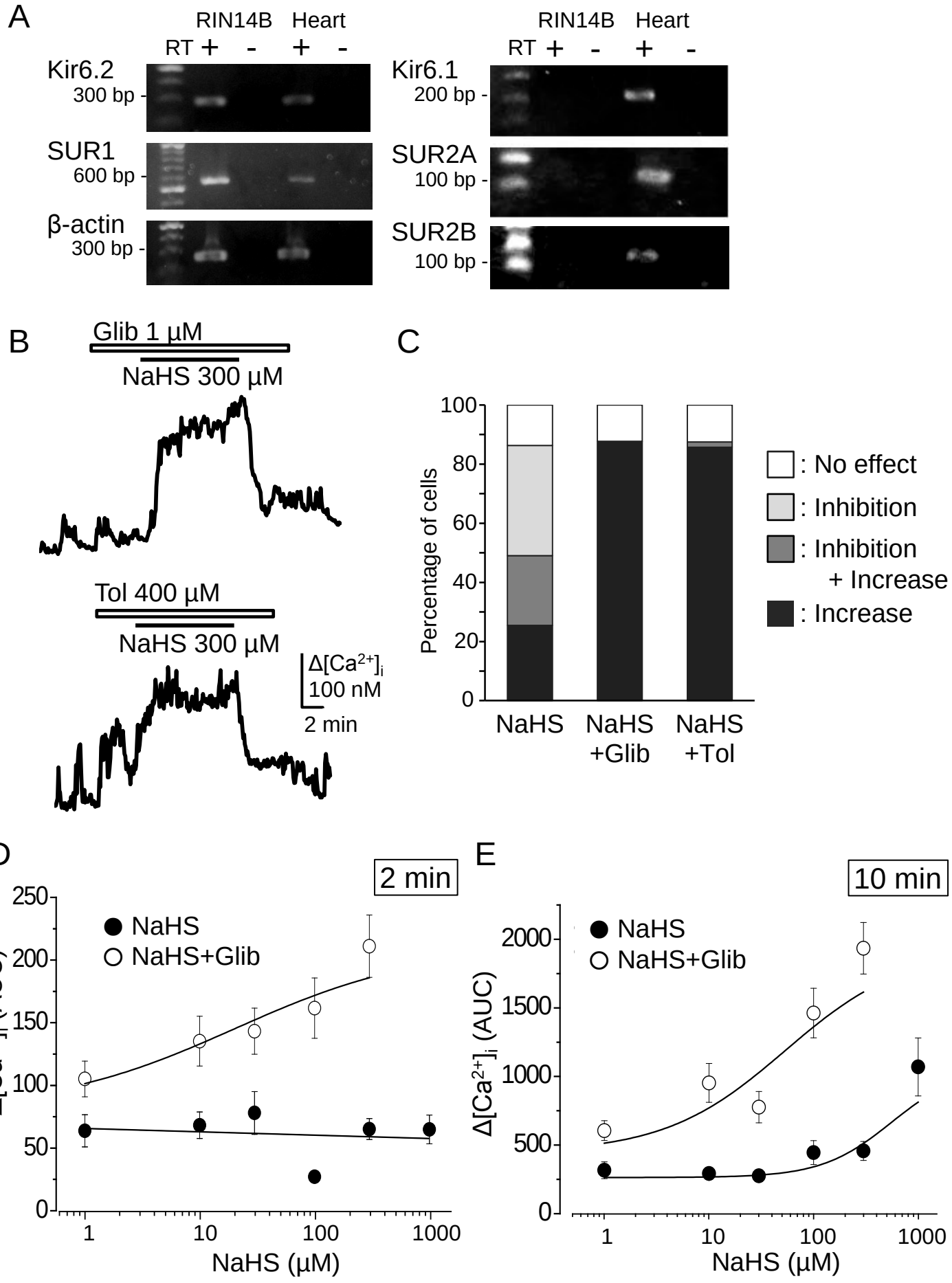
A
RIN14B
Heart
RT + - + -
Kir6.2
300 bp
SUR1
600 bp
β-actin
300 bp
Kir6.1
200 bp
SUR2A
100 bp
SUR2B
100 bp
B
Glib 1 μM
NaHS 300 μM
Tol 400 μM
NaHS 300 μM
Δ[Ca2+]i
100 nM
2 min
C
Percentage of cells
: No effect
: Inhibition
: Inhibition + Increase
: Increase
NaHS
NaHS +Glib
NaHS +Tol
D
2 min
NaHS
NaHS+Glib
Δ[Ca2+]i (AUC)
NaHS (μM)
E
10 min
NaHS
NaHS+Glib
Δ[Ca2+]i (AUC)
NaHS (μM)

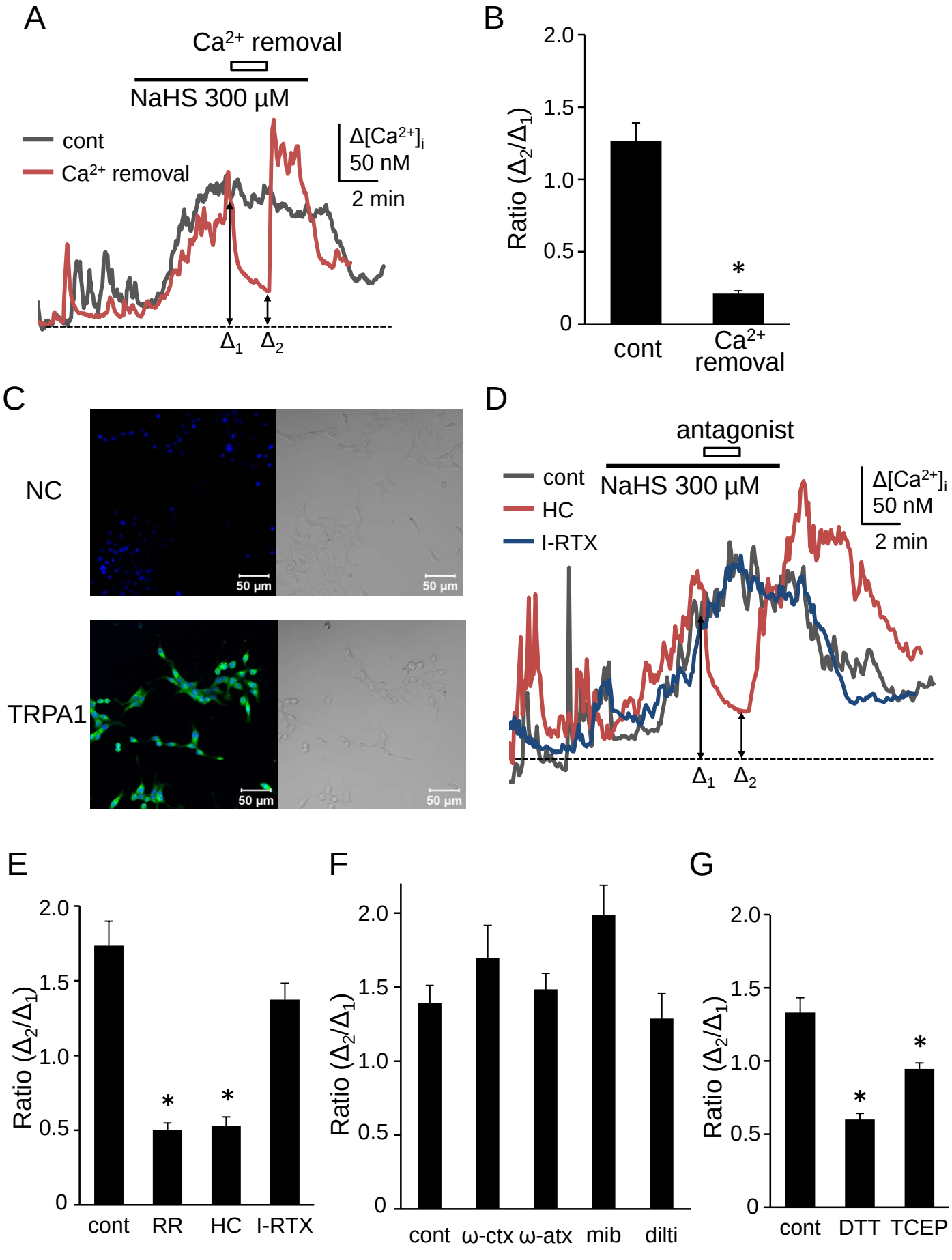
A
Ca2+ removal
NaHS 300 µM
cont
Ca2+ removal
Δ[Ca2+]i
50 nM
2 min
Δ1
Δ2
B
Ratio (Δ2/Δ1)
2.0
1.5
1.0
0.5
0
*
cont
Ca2+ removal
C
NC
TRPA1
50 µm
50 µm
50 µm
50 µm
D
antagonist
NaHS 300 µM
cont
HC
I-RTX
Δ[Ca2+]i
50 nM
2 min
Δ1
Δ2
E
Ratio (Δ2/Δ1)
2.0
1.5
1.0
0.5
0
*
*
cont
RR
HC
I-RTX
F
Ratio (Δ2/Δ1)
2.0
1.5
1.0
0.5
0
cont
ω-ctx
ω-atx
mib
dilti
G
Ratio (Δ2/Δ1)
2.0
1.5
1.0
0.5
0
*
*
cont
DTT
TCEP

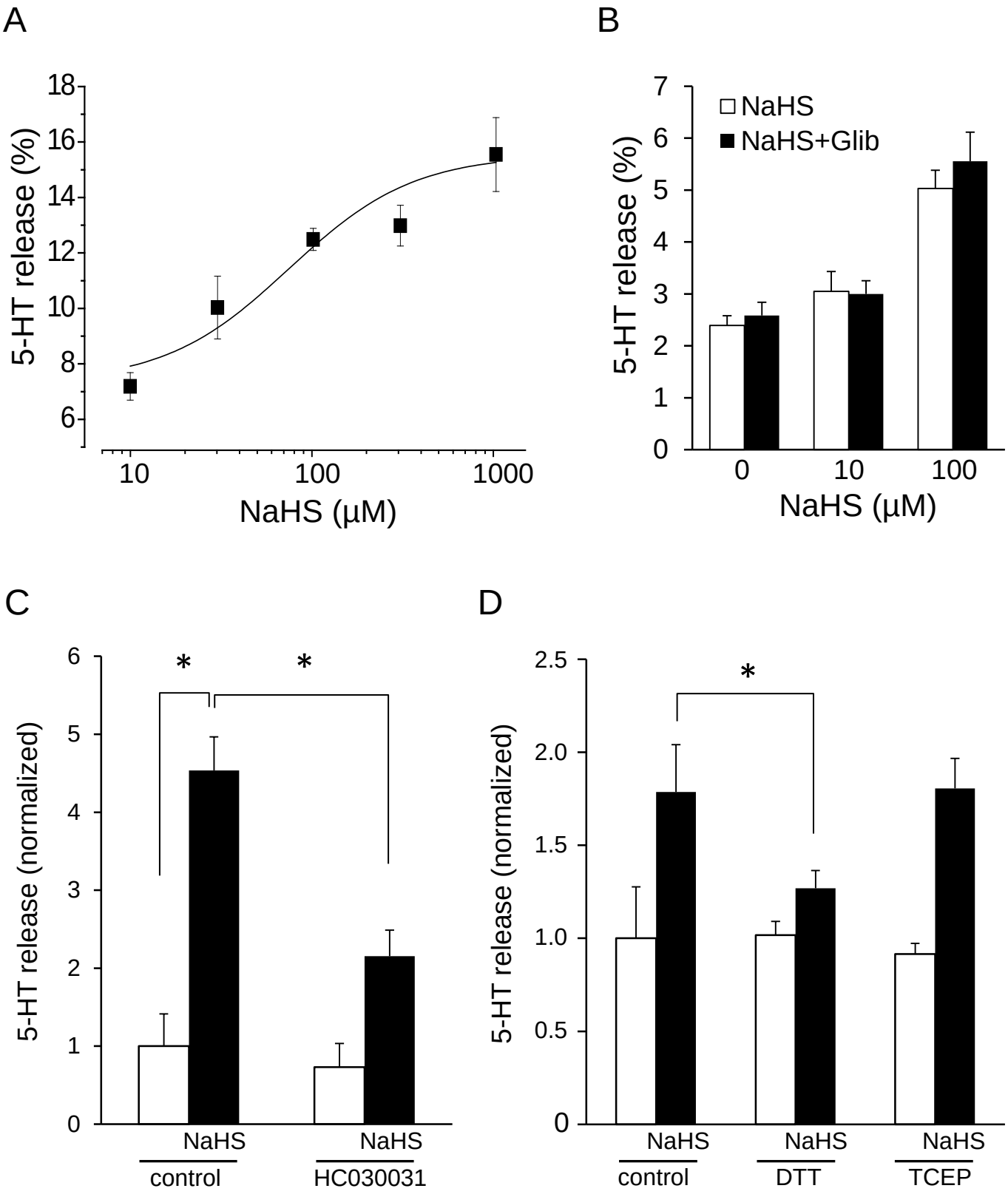
A
5-HT release (%)
18
16
14
12
10
8
6
10
100
1000
NaHS (μM)
B
NaHS
NaHS+Glib
5-HT release (%)
7
6
5
4
3
2
1
0
0
10
100
NaHS (μM)
C
5-HT release (normalized)
6
5
4
3
2
1
0
*
*
NaHS
NaHS
control
HC030031
D
5-HT release (normalized)
2.5
2.0
1.5
1.0
0.5
0
*
NaHS
NaHS
NaHS
control
DTT
TCEP